



# Impact of Different Grain Refiner Addition Ratios on the Microstructural Properties of 6082 Aluminum Alloy

B. Tunca\* , B. Ince , D. Deniz 

Sistem Alüminyum San. ve Tic. A.Ş., Turkey

\* Corresponding author: E-mail address: bilgehantnca@gmail.com

Received 22.07.25; accepted in revised form 25.09.25; available online 09.03.2026

## Abstract

This study examines the impact of grain refiners on the microstructural properties of 6082 aluminum alloy, emphasizing the effect of varying addition rates on grain size and refinement efficiency. Four grain refiners (GR1, GR2, GR3, GR4) were tested at different rates, with results assessed through chemical composition analysis, microstructural examination, and grain size measurements. The findings reveal that lower addition rates proved more effective: for instance, GR3 at 0.33 kg/t achieved a grain size of 110  $\mu\text{m}$ , while at 0.76 kg/t it reached 105  $\mu\text{m}$ ; GR4 achieved comparable grain sizes (131  $\mu\text{m}$  at 0.30 kg/t) with high efficiency. In contrast, higher rates (e.g., GR1 and GR2 at 1.48-1.53 kg/t) yielded lower efficiency despite smaller grain sizes. These findings suggest that excessive addition rates are redundant, with optimized lower rates yielding finer grains and higher efficiency. Chemical analysis confirmed that changes in Ti and B concentrations aligned with addition rates, yet lower rates offered superior recovery and effectiveness. Microstructural analysis further demonstrated that GR3 and GR4 at reduced rates produced homogeneous, fine-grained structures, enhancing casting quality and cost-effectiveness. This study highlights that optimizing grain refiner addition rates enhances microstructural control and economic efficiency in 6082 alloy casting. Future research should focus on fine-tuning these rates and exploring alternative refinement techniques to further improve the mechanical properties and castability of aluminum alloys. This study uniquely demonstrates that optimized low addition rates enhance microstructural homogeneity while providing significant cost and environmental benefits, addressing a critical gap in industrial grain refinement practices.

**Keywords:** Grain refinement, Microstructure, Grain size, 6082 alloy, Al-Ti-B

## 1. Introduction

Aluminum is the second most abundant metallic element in the Earth's crust and is widely used in engineering applications due to its lightweight nature, high strength, and resistance to corrosion. Aluminum alloys, which can have their mechanical properties enhanced through heat treatment, are distinguished by their low melting point and specific gravity. Aluminum alloys, made with added elements, are commonly used in aerospace and automotive fields. [1-4].

With the continuous expansion of application areas for aluminum alloys, significant requirements have emerged regarding the control of their microstructure. Grain size and morphology, key characteristics of the microstructure of aluminum alloys, directly impact material performance. An ideal microstructure should consist of fine and uniform isometric crystal grains, contributing to overall performance improvement [5]. Additionally, refinement techniques are an effective method used to influence grain formation and reduce oxide compounds at grain boundaries [6,7].

In alloy castings, the objective is generally to achieve a fine, uniformly sized grain structure to improve the material's durability



and quality. In the casting of aluminum alloys, the inoculation method is widely used to obtain this fine-grained structure. Inoculation ensures a more homogeneous and higher-quality material during casting. Among the various options available, the grain refiners most frequently employed in the production and enhancement of aluminum alloys are the Al-Ti-B master alloys, valued for their effectiveness in improving structural properties [8,9].

In cast aluminum alloys, grain structure is a highly significant and easily observable property. Grain morphology can appear in three different forms: columnar, twinned columnar, and equiaxed grains. Specialized inoculants, widely recognized as grain refiners, play a crucial role in obtaining a uniform equiaxed grain structure within the material, and these are generally introduced during the process in the form of carefully formulated master alloys to ensure optimal results [10,11].

Grain refinement in aluminum is achieved through heterogeneous nucleation by adding particles to the molten metal. This process prevents issues such as hot cracking during casting, improves surface quality, and reduces porosity. Grain refinement aims to achieve fine, equiaxed grains to enhance casting quality and mechanical properties. However, in some cases, larger and uniform grains may be preferred to prevent crack propagation. Effective grain refinement is considered successful when the grain diameter is less than approximately 200  $\mu\text{m}$ . Grain refinement in aluminum and its alloys is a widespread industrial practice, as it ensures the formation of uniformly sized grains during solidification. Moreover, studies in this field over the past 50 years have focused not only on developing effective grain-refining agents but also on understanding the mechanisms of the grain refinement process [12,13].

Al-Ti-B alloys are widely used master alloys for grain refinement in aluminum castings and have significant industrial applications. Their production is typically carried out by reacting inorganic salts such as potassium fluor titanate ( $\text{K}_2\text{TiF}_6$ ) and potassium fluoroborate ( $\text{KBF}_4$ ) with aluminum at temperatures between 700°C and 800°C. The resulting product is an Al-Ti-B alloy formed under a KF-AlF<sub>3</sub>-based flux. The incorporation of master alloys for grain refinement is a standard practice widely adopted in commercial foundries to enhance material properties. Among these, aluminum master alloys that combine titanium and boron in their formulations stand out as particularly popular choices, having been specially designed and optimized to meet the needs of wrought alloys in various industrial applications [14,15].

Zhang et al. (2025) comprehensively reviewed grain refinement methods for aluminum alloys. They classified techniques into chemical (alloying elements, grain refiners, nanoparticles), physical (thermal control, mechanical, and electromagnetic methods), and composite approaches, discussing their advantages and limitations. They highlighted that Ti, B, and rare earth elements promote heterogeneous nucleation, while Al-Ti-B and Al-Ti-C master alloys are widely used but face issues like poisoning and preparation challenges. Nanoparticles and composite methods show promise for high-performance alloys. The authors also elucidated refinement mechanisms (e.g., encapsulation reaction, free growth model) and provided directions for future research [5].

Li et al. (2021) conducted a detailed examination of the nucleation process of  $\alpha$ -Al on TiB<sub>2</sub> particles within Al-Cu alloys,

focusing on the atomic-level interactions. Their findings highlighted that the Al<sub>5</sub>Ti layer, which emerges due to titanium segregation along the basal plane of TiB<sub>2</sub> particles, serves as a pivotal factor in facilitating the nucleation of  $\alpha$ -Al, significantly influencing the alloy's microstructural development. It was also noted that in cases of high Cu concentration, a Cu-rich layer forms, influencing the nucleation process [16].

Guan et al. (2017) comprehensively reviewed grain refinement techniques in aluminum alloys, categorizing them into four main groups: vibration and stirring during solidification, rapid solidification, grain-refining additives, and severe plastic deformation. The study detailed the mechanisms, advantages, and disadvantages of each method. It highlighted the effectiveness of additives like Al-Ti-B in grain refinement and the role of severe plastic deformation techniques such as ECAP and HPT in producing ultra-fine-grained structures. It has been suggested that future research should focus on developing more efficient, cost-effective, and environmentally friendly grain refinement techniques [17].

Sigworth and Kuhn (2007) explored a wide range of grain refinement methods applied to aluminum casting alloys, placing particular emphasis on the benefits offered by contemporary Al-Ti-B grain refiners. Their research revealed that boron outperforms titanium as a grain refiner and that maintaining lower titanium concentrations can enhance mechanical properties while also improving resistance to hot cracking in certain alloy compositions. Furthermore, the study outlined optimal grain refinement strategies tailored to various alloy systems, providing practical guidance for foundry applications. Notably, it was pointed out that a minimal boron addition ranging from 10 to 20 parts per million proves adequate for Al-Si alloys, whereas Al-Si-Cu alloys require a titanium content of at least 0.1% to achieve effective results [18].

Jones and Pearson (1976) delved deeply into the impact of incorporating titanium and boron on the grain refinement process of aluminum alloys, offering an in-depth exploration of the subject. They substantiated the efficacy of Al-Ti-B master alloys in achieving grain refinement through a combination of detailed thermodynamic analysis and robust experimental evidence, providing a solid foundation for their conclusions. The phase diagrams and solubility data presented in the article serve as an important resource for understanding the behavior of alloys during the grain refinement process. It was also noted that certain alloying elements (e.g., zirconium and chromium) may reduce grain refinement effectiveness, with the thermodynamic reasons for this phenomenon explained. This study provides a significant contribution to research on the grain refinement of aluminum alloys [19].

Izcan Kurtaran et al. (2021) meticulously investigated how grain refinement influences the mechanical characteristics of the AA 6082 aluminum alloy, which belongs to the Al-Mg-Si family of alloys. Their study involved introducing different quantities of the AlTi<sub>5</sub>B<sub>1</sub> grain refiner to the alloy, followed by a series of carefully controlled processes including casting, homogenization, and artificial aging to optimize its properties. Through detailed microstructure analysis and rigorous mechanical testing, they discovered that adding 0.11% AlTi<sub>5</sub>B<sub>1</sub> led to a remarkable 69% decrease in grain size alongside a substantial 17% enhancement in mechanical strength. Additionally, their findings indicated that incorporating elements like magnesium (Mg) and chromium (Cr)

further contributed to reducing grain size while simultaneously boosting the alloy's overall strength [20].

Easton et al. (2016) reviewed recent advancements in grain refinement of light metals and alloys (aluminum, magnesium, titanium). They highlighted that grain refinement reduces hot tearing, disperses porosity, and enhances mechanical properties. Theoretical models, such as the Interdependence Theory and Free Growth model, were discussed, addressing the interplay between nucleation and growth restriction (Q factor). Chemical (inoculants, solutes), physical (ultrasonic treatment, electromagnetic fields), and composite methods were examined, with contributions from advanced experimental techniques like synchrotron X-ray observations emphasized. New grain refiners, such as Al-Nb-B and oxide-based refiners for Al-Si alloys, were introduced, though challenges in refining magnesium and titanium alloys persist [21].

Zhao et al. (2019) investigated the effects of adding Al-5Ti-x(Mg-30%Ce) grain refiner on the microstructure, hardness, tensile, and impact properties of Al-7Si alloy. The study found that Mg-30%Ce enhanced the refinement effect of Al-5Ti, refining both  $\alpha$ -Al and eutectic Si. The most significant refinement was observed with 2% Mg-30%Ce, reducing grain size from 129  $\mu\text{m}$  to 90  $\mu\text{m}$ . Hardness, tensile strength, and impact toughness improved; with 2% Mg-30%Ce, tensile strength reached 256 MPa, and impact toughness increased to 34.91 J/cm<sup>2</sup>, a 78.7% improvement over Al-5Ti alone. Split Hopkinson Pressure Bar (SHPB) tests revealed significant strain rate sensitivity at high strain rates ( $\geq 2.0 \times 10^3 \text{ s}^{-1}$ ), with the 2% Mg-30%Ce specimen showing the best impact resistance. Improvements were attributed to the refinement of TiAl<sub>3</sub> phase, transformation of eutectic Si to granular morphology, and increased grain boundaries hindering dislocation movement [22].

Li et al. (2023) explored the relationship between microstructure configuration and mechanical properties of an Al-7Si-0.4Mg alloy refined with C-doped TiB<sub>2</sub> (C-TiB<sub>2</sub>) and reinforced with SiC. Using Al-TCB-25Si master alloy, the average grain size of the cast alloy was refined to 69.2  $\mu\text{m}$ , further reduced to 36.7  $\mu\text{m}$  after hot extrusion. In the cast (AN) alloy, eutectic Si and reinforcing particles formed a network configuration, while in the extruded (AS) alloy, they aligned in a streamlined distribution along the extrusion direction. The network configuration provided higher strength, whereas the streamlined configuration nearly doubled ductility. After T6 heat treatment, the AN alloy achieved an ultimate tensile strength (UTS) of 338 MPa and yield strength (YS) of 275 MPa, while the AS alloy reached 329 MPa UTS and 267 MPa YS with higher elongation (15.2%). Nano-Al precipitates and Si twins enhanced the toughness of eutectic Si, inhibiting crack propagation. Strength improvements were attributed to grain refinement, the network configuration of eutectic Si, and nano-precipitates hindering dislocation movement, while increased ductility was linked to the streamlined configuration facilitating matrix deformation and hindering crack connectivity [23].

Prema et al. (2019) investigated the effects of grain refiners (Al-5Ti-1B, Al-3B) and a modifier (Al-10Sr) on the microstructure and mechanical properties of commercial Al-Si eutectic alloy LM6 (12% Si). Master alloys Al-5Ti-1B (0.2 wt%), Al-3B (1 wt%), and Al-10Sr (0.3 wt%) were added individually and compared with the untreated alloy. Addition of Al-5Ti-1B resulted in a fully equiaxed, finer-grained microstructure with no columnar grains observed. Mechanical tests showed that Al-3B addition improved turning and surface roughness performance (better force acceptance and

surface finish), while Al-5Ti-1B enhanced drilling performance with higher thrust resistance. Al-10Sr increased ultimate tensile strength (UTS) and wear resistance, with untreated LM6 and Al-10Sr-treated alloy exhibiting high hardness values. SEM micrographs confirmed that grain refiners and the modifier refined eutectic Si and promoted a more uniform distribution. The results indicate that finer grain sizes enhance mechanical properties, and the properties of Al-Si alloys are governed by microstructural features [24].

Zhang et al. (2017) investigated the effectiveness of an in-situ synthesized Al<sub>2</sub>.2Ti1B-Mg master alloy for grain refinement of A356 Al-Si alloy. The master alloy was prepared via a two-step chemical reaction, forming TiB<sub>2</sub> particles and magnesium aluminate (MgAl<sub>2</sub>O<sub>4</sub>) phase. Experiments showed that A356 alloy treated with Al<sub>2</sub>.2Ti1B-Mg achieved fine equiaxed grains. The  $\alpha$ -Al grain size was reduced from 950  $\pm$  135  $\mu\text{m}$  in the untreated alloy to 620  $\pm$  95  $\mu\text{m}$  with Al5Ti1B and to 320  $\pm$  50  $\mu\text{m}$  with Al<sub>2</sub>.2Ti1B-Mg. After T6 heat treatment, the alloy refined with Al<sub>2</sub>.2Ti1B-Mg exhibited a yield strength (YS) of 257  $\pm$  5 MPa, ultimate tensile strength (UTS) of 313  $\pm$  5 MPa, and elongation of 7.8  $\pm$  0.5%, representing increases of 14 MPa, 8 MPa, and 1% respectively compared to Al5Ti1B. The elongation doubled compared to the untreated alloy. The formation of MgAl<sub>2</sub>O<sub>4</sub> on TiB<sub>2</sub> surfaces provided low lattice misfit (1.11%) for  $\alpha$ -Al nucleation, enhancing refinement efficiency. This demonstrates that Al<sub>2</sub>.2Ti1B-Mg is more effective and stable than Al5Ti1B and Al3Ti3B as a grain refiner. Improved mechanical properties were attributed to refinement strengthening [25].

Beyond Al-Ti-B, alternative grain refiners such as Al-Nb-B and oxide-based refiners for Al-Si alloys have shown promise, though their application in wrought alloys like AA6082 remains limited [21]. This study addresses this gap by systematically evaluating Al-Ti-B refiners at low addition rates, offering a cost-effective solution for industrial applications.

This study aims to systematically investigate the performance of commercially available grain refiners in 6082 aluminum alloys, focusing on the effects of varying addition rates on chemical composition, grain size, and grain refinement efficiency. Aluminum alloys, valued for their lightweight properties, high strength, and corrosion resistance, are widely utilized in aerospace, automotive, and other industrial applications. However, controlling the microstructure, particularly grain size and morphology, is critical to optimizing the mechanical properties and casting quality of these alloys. In this context, the primary objective of this study is to evaluate the efficacy of Al-Ti-B-based grain refiners in 6082 aluminum alloys, determine optimal addition rates to achieve finer and more uniform grain structures, and propose more efficient and cost-effective methods for industrial casting processes.

The motivation for this study stems from the challenges encountered in grain refinement during aluminum alloy casting and the need to optimize existing methods. While the literature demonstrates that grain refinement techniques, such as the use of Al-Ti-B master alloys, enhance mechanical properties and reduce casting defects, further research is needed to understand the impact of addition rates and the comparative performance of different grain refiners. Specifically, the hypothesis that lower addition rates can achieve high grain refinement efficiency holds significant potential for both cost-effectiveness and environmental sustainability. This study seeks to contribute to the optimization of

grain refinement processes by analyzing the performance of various grain refiners (GR1, GR2, GR3, GR4) in both laboratory and industrial settings. Additionally, by examining the relationship between grain size and chemical composition, as well as calculating refinement efficiencies, this work aims to address knowledge gaps in the literature and foster innovative approaches to enhance the mechanical properties of aluminum alloys.

Unlike previous studies focusing on high addition rates, this work uniquely investigates the efficacy of minimal addition rates, revealing their potential to achieve superior microstructural control with reduced material consumption.

## 2. Material and Method

The casting of the 6082 aluminum alloy was carried out using a direct water-cooled vertical casting system shown in Figure 1. In this system, during the casting preparation stage, the starter heads are inserted into the mold and aligned with each other. Before casting begins, water is supplied to the casting table, initiating continuous cooling of the mold through internal water flow. Once the molten metal enters the casting table, it is allowed to fill the top of the starter heads. At this stage, to prevent the solidification front from rising into the casting table and to maintain solidification at the mold level, the casting process is started in a downward direction. Continuous flow of molten metal into the casting table ensures the progressive growth of the billets, and the process continues in this manner until the desired casting length is achieved.

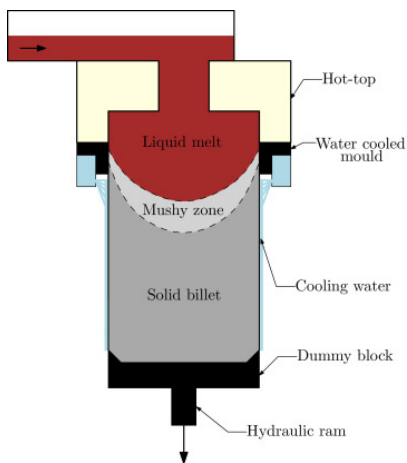


Fig. 1. Schematic of Direct-Chill Vertical Casting system [26]

In this type casting process, temperature of melted metal in furnace, flow of water ( $\text{m}^3/\text{h}$  or  $\text{l}/\text{min}$ ), temperature of water and casting speed are the most important parameters. Casting parameters can be changed depends on the alloy type and diameter of billet. In generally 7" 6082 alloy casting parameters are casting table temperature  $685^\circ\text{C}$ , the water flow between the 5000-6000  $\text{l}/\text{min}$ . and casting speed between the 110-120  $\text{mm}/\text{min}$ .

In this study, the functioning of commercially available grain refiners in 6082 aluminum alloys was investigated. The effect of the grain refiner currently used in our foundry was examined across

four different castings, with the results presented in Tables 1, 2, and 3. The addition rates and changes in grain size were analyzed here. Subsequently, a specific alloy was selected in a laboratory setting, and different grain refiners were added to this alloy in varying proportions to study their efficiency and effects.

Casting experiments were conducted at a pouring temperature of  $720 \pm 10^\circ\text{C}$ , with grain refiners added during casting to ensure homogeneous dispersion. Addition rates (0.30–1.53  $\text{kg}/\text{t}$ ) were selected based on industrial standards (1.5  $\text{kg}/\text{t}$  for AA6082) and preliminary trials to evaluate the efficacy of reduced rates, aiming to optimize cost and efficiency.

### 2.1. Chemical Analysis

In the study, chemical composition analysis were conducted using the ARTUS 8 spectrometer analysis device. The values shown in Table 1 and Table 2 are calculated based on the results of the chemical composition analysis. The range of addition rates was selected to include values both below and above the typical industrial rate of 1.5  $\text{kg}/\text{t}$ , enabling a comprehensive evaluation of grain refinement efficiency with minimal material usage. Examinations and preliminary studies of different 6082 alloy castings, as presented in Tables 1 and 2, were conducted. Grain refiners with a Ti/B ratio of 5/1 were analyzed, as detailed in Tables 1 and 2. The results from the chemical analysis on Ti and B are shown in table 1 and the recovery calculated from changes in Ti and B are summarized in Table 2. Given that a 5/1 Ti/B grain refiner is used, a 1  $\text{kg}/\text{t}$  addition is expected to increase the Ti concentration by 50 ppm and the B concentration by 10 ppm.

In summary, the recovery values show that the particles forming the nucleus in the casting systems are not lost. If the particles pass to the casting table with a high addition rate, there will be no problem even when the additions are reduced to very low levels.

### 2.2. Microstructure Analysis

Furnace sample for microstructure analysis is taken from the melted aluminium from the furnace shown in Figure 2. It is solidified in the copper mold which developed for billet casting solidification simulation. In the past experiences, microstructure of this type samples of grain size is between the  $\pm 5 \mu\text{m}$  compared the billet disc sample. Solidification of the furnace sample likes the billet casting parameters. Sample is cutted two pieces and cutted again for microanalysis specimen which taken from the centre of the sample.

Table 1.

The production addition rates are calculated from production parameters. Analysis values are given as ppm, 1 ppm = 0.0001 %.

Castings	Element	Furnace (ppm)	Feeding Addition Rate (kg/t)	Chemical Analysis Ti Cont. (ppm)	Chemical Analysis B Cont. (ppm)	Castings (ppm)
Cast-1	AlTiB		1.1200			
	Ti	118	0.0560	64.0		182.0
	B	4.6	0.0112		11.4	16.0
Cast-2	AlTiB		0.8200			
	Ti	94	0.0410	24		118.0
	B	4.2	0.0082		5.2	9.4
Cast-3	AlTiB		1.1200			
	Ti	163	0.0560	56		219.0
	B	9.7	0.0112		9.7	19.4
Cast-4	AlTiB		1.5100			
	Ti	154	0.0755	103		257.0
	B	10.9	0.0151		15.5	26.4

Table 2.

Recoveries from addition rates calculated from changes in Ti and B concentrations, see table 1.

Castings	Element	Feeding Addition Rate (kg/t)	Furnace (ppm)	Calculated Sample Concentration (ppm)	Casting Sample Concentration (ppm)	Recovery (%)
Cast-1	AlTiB	1.1200				
	Ti	0.0560	118	174	182	104,60%
	B	0.0112	4.6	15.8	16.0	101,27%
Cast-2	AlTiB	0.8200				
	Ti	0.0410	94	135	118	87,41%
	B	0.0082	4.2	12.4	9.4	75,81%
Cast-3	AlTiB	1.1200				
	Ti	0.0560	163	219.0	219	100%
	B	0.0112	9.7	20.9	19.4	92,82%
Cast-4	AlTiB	1.5100				
	Ti	0.0755	154	229.5	257	111,98%
	B	0.0151	10.9	26.0	26.4	101,54%



Fig. 2. Furnace sample for microanalysis

Casting sample for microstructure analysis is cutted from the billet with disk formation shown in Figure 3. Cutted specimen from the centre billet disc is bakelited. Then, the surface is sanded with sandpaper in three different abrasive sizes. Then, polishing process is carried out. Finally, etching process is carried out with HF and

Barker solutions for grain size examination. The grain size analysis was conducted using the Nikon Eclipse MA200 device.

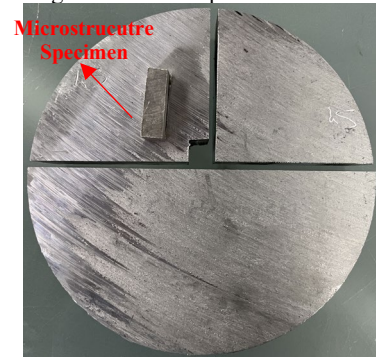


Fig. 3. Microstructure specimen from the casted billet.

In Table 3, the grain sizes of the four castings performed were examined. In this process, samples are cut from the areas to be examined.

Table 3.

Grain size measurements on samples

	Furnace	After Grain Refiner	After Filter
	Grain Size( $\mu\text{m}$ )	Grain Size( $\mu\text{m}$ )	Grain Size( $\mu\text{m}$ )
Cast-1	218	121	115
Cast-2	169	140	143
Cast-3	169	107	111
Cast-4	199	109	102

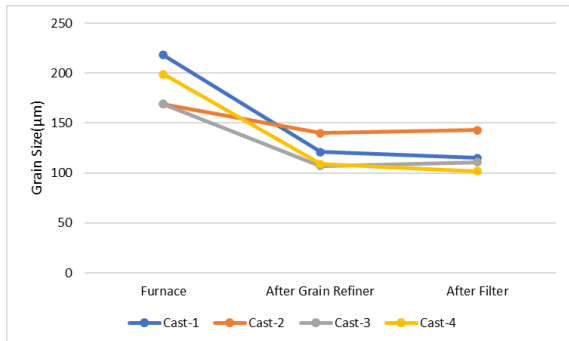


Fig. 4. Changes in Grain Size of Samples Taken During Casting

In Figure 4, the variations observed in grain size, based on a detailed set of measurements systematically carried out to monitor the condition of the castings, are comprehensively presented. The initial sample was extracted from the liquid metal in the furnace just moments before the casting process began. The second sample was subsequently obtained immediately after the grain refiner was carefully incorporated into the molten mixture. The following sample, taken after the filtration process had fully concluded, completes the sequence. The grain size measurements align with the expected trends based on addition rates, as shown in Tables 1 and 2. As seen in Tables 1 and 2, different amounts of additions were made, and the effectiveness of the existing grain refiner was evaluated. The best grain size results in percentage terms were obtained in Cast-4, where the addition rate was a high addition rate of 1.51 kg/t.

The grain sizes at the casting table are small. The grain sizes in furnace samples have been correlated to billet grain sizes at many cast houses. The standard positions to measure billet grain size is either 25-30 mm from billet surface or at mid-radius. The difference between billet grain size and furnace sample grain size lies between 40-70  $\mu\text{m}$ , depending on billet diameter. This means that the billet grain sizes for the actual casts are between 60-90  $\mu\text{m}$ , if measured at the positions given above.

The center of the billet should be avoided for grain size measurements. The grain size can be very inhomogeneous, since this is the sump region, where crystals may occur that have been nucleated long before the solidification front reaches the center.

### 2.3. Grain Refiner Efficiency

The outcomes derived from experiments involving grain refiners are generally represented in terms of a singular grain size

value, and these refiners are categorized according to the differences in grain size that become apparent when maintaining a consistent addition rate. Within the scope of this research, particular emphasis has been placed on analyzing the volume occupied by the grains, whereby the quantity of grains present within a specified unit of volume is directly related to and evaluated in relation to the precise amount of boron introduced into the system during the process. Research conducted by Greer and his team has established that the most efficient shape for filling a three-dimensional space is a tetrakaidecahedron, a polyhedron with 14 faces [27]. Based on this finding, a mathematical formula has been derived to relate the number of grains to the grain size measured using the intercept method:

$$N_V \approx \frac{0.5}{L^3} \quad (1)$$

Within this equation,  $N_V$  symbolizes the total number of grains contained within a given unit of volume, whereas  $L$  stands for the line intercept length, which, for the sake of uniformity and clear understanding, has been deliberately expressed in millimeters throughout the study. Consequently, the grain count is calculated per cubic millimeter ( $\text{mm}^3$ ). Provided that every aluminum grain originates through nucleation triggered by a boride particle,  $N_V$  serves not only as a measure of the number of grains per unit volume but also as an indicator reflecting the total quantity of effective boride particles present and actively contributing within the material. To evaluate the efficiency of grain refiners, this value is divided by the boron concentration, measured in parts per million (ppm B). This method enables a systematic analysis and comparison of the effectiveness of grain refiners across different addition rates:

$$Efficiency = \frac{\frac{\text{Number of grains}}{\text{mm}^3}}{\text{Added ppm B}} \quad (2)$$

This equation connects the number of active boride particles, each contributing to the formation of an aluminum grain, to the total mass of boride material incorporated into the alloy. When the scope of the analysis is expanded, more detailed insights emerge regarding how boron content influences the microstructure, providing a practical foundation for optimizing grain refinement processes using measurable data. This approach not only highlights the performance of the refiners but also offers greater understanding of the fundamental mechanisms driving grain formation under varying boron levels.

## 3. Experiment and Optimization Results

In this study, a 6082 alloy was cast, and experiments were conducted on it. A product cast without grain refiner was remelted on a smaller scale, and four different grain refiners were added at varying rates, resulting in a total of eight trials. These trial castings were poured as furnace samples, and their chemical compositions and grain structures were analyzed to measure the efficiency of the grain refiners. GR1-2-3-4 were selected based on their commercial

availability and varying Ti/B ratios to assess their efficacy across a broad spectrum.

### 3.1. Chemical Analysis

As mentioned in the section above, targeting this casting analysis, different grain refiner products were added at varying rates to the castings, and their analysis were conducted. The %Ti value here is 0.017. In the study, efforts were made to reduce this value further by adding smaller amounts of different products. Even though the values in the chemical composition appeared lower, changes in grain sizes were still observed.

Table 4 compares the chemical composition of the cast AA6082 alloy with furnace samples. The slight reduction in Ti (0.017% to 0.010%) and Mg (0.80% to 0.77%) in furnace samples is attributed to minor losses during remelting and casting, while Fe and Cu levels remain consistent, confirming compositional stability across the trials. The chemical compositions provided in Table 4 were remelted and cast with varying amounts of Al-Ti-B added in the GR1, GR2, GR3, and GR4 castings.

Table 4. Chemical Composition of the 6082 Alloy

Alloy	Fe (%)	Si (%)	Cu (%)	Mn (%)	Mg (%)	Zn (%)	Ti (%)
AA6082	0.25	0.83	0.055	0.54	0.80	0.07	0.017
Furnace	0.27	0.82	0.059	0.50	0.77	0.05	0.010

### 3.2. Grain Refiner Efficiency

Grain size measurements were conducted in accordance with ASTM E112-13, using the intercept method on a Nikon Eclipse MA200 microscope [28]. For each casting, at least five regions were analyzed, and the standard deviation ( $\sigma$ ) was calculated to quantify grain size variance. For instance, GR3-A exhibited an average grain size of 110  $\mu\text{m}$  with a standard deviation of  $\pm 8 \mu\text{m}$ , indicating a range of 102–118  $\mu\text{m}$ . These variances were incorporated as error bars in Figure 5, reflecting measurement uncertainty and casting variability. Grain size measurements adhered to ASTM E112-13, ensuring standardized and reproducible results [28]. The correlation between furnace and billet grain sizes (40–70  $\mu\text{m}$  difference) was considered, with measurements taken at standard positions (25–30 mm from the billet surface or mid-radius). For standard castings of AA6082, the typical addition rate is 1.5 kg/t. In this study, four different grain refiners were used, and different addition rates were determined. These four distinct castings are labeled GR1, GR2, GR3, and GR4. Within each, they are classified as A and B based on the addition rates. Test results are shown in Table 5 and Figure 5. Figure and Figure 6 complement Table 5 by visually representing grain size and efficiency trends, respectively, to facilitate interpretation of the data.

Table 5. Grain Refinement Test in AA6082 Alloy

Cast Name	Addition Rate (kg/t)	Grain Size ( $\mu\text{m}$ )	Efficiency (grain/mm <sup>3</sup> /ppm B)
GR1-A	0.75	142	23
GR1-B	1.48	124	18
GR2-A	0.76	159	16
GR2-B	1.53	135	13
GR3-A	0.33	110	92
GR3-B	0.76	105	51
GR4-A	0.30	131	69
GR4-B	0.78	124	36

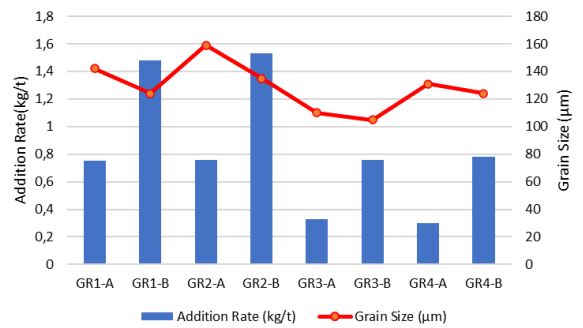


Fig. 5. Graph Showing the Correlation Between Addition Rate and Resulting Grain Size Changes

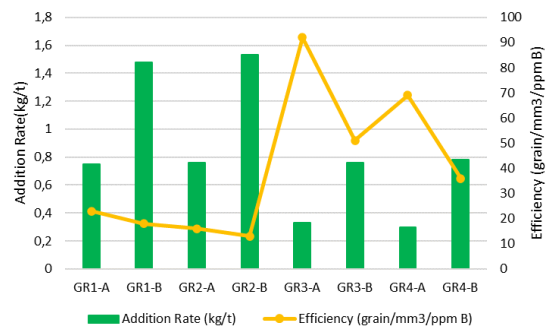


Fig. 6. Graph Showing the Correlation Between Addition Rate and Efficiency

In the casting experiments conducted with different grain refiners, the addition rates, grain sizes, and efficiencies were calculated and presented in Table 5. As shown in Figure 5, although the addition rates for GR1 and GR2 products are high, their efficiencies are low. In the case of GR3 and GR4 castings, although the addition rates used are lower, the grain sizes are similar or even smaller. The GR3 refiner, particularly at 0.33 kg/t (GR3-A), achieved a grain size of 110  $\mu\text{m}$  with superior efficiency (92 grains/mm<sup>3</sup>/ppm B). When an addition rate of 0.33 kilograms per ton was applied, the resulting grain size measured 110 micrometers, whereas with an increased addition rate of approximately 0.76 kilograms per ton, the grain size was observed to reduce slightly, reaching a value of around 105 micrometers. In this context, it was determined that a double addition was unnecessary, and the 0.33 addition was sufficient for controlling

grain size. Figure 6 shows the graph depicting the relationship between addition rate and efficiency. The highest efficiency was found in the GR3 and GR4 castings. The best efficiencies were achieved in GR3-A and GR4-A, with the results indicating that GR3-A delivered the best outcomes.

### 3.3. Microstructure Analysis

The grain structure analysis of GR1 and GR2 castings is provided in Figure 7.

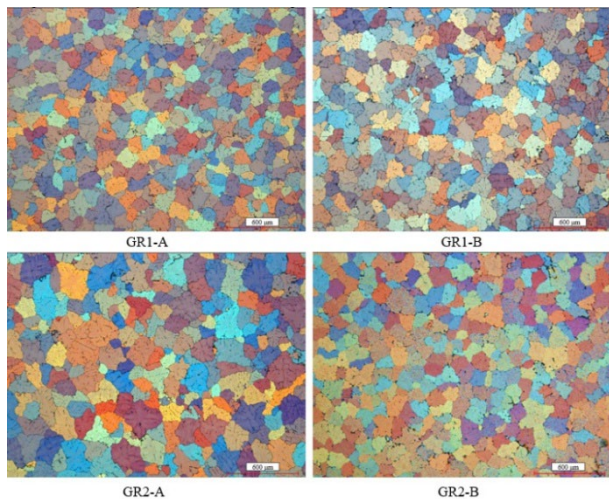


Fig. 7. Microstructure Images of GR1 and GR2 Castings

The grain size analysis of GR3 and GR4 castings is provided in Figure 8.

In the grain size analysis, it was observed that when GR1 and GR2 were used in high amounts, there was a decrease in grain size, but when efficiencies were calculated, they were found to be low. In contrast, in the GR3 and GR4 castings, similar grain sizes were measured by using smaller amounts, which is why their efficiencies are higher. The highest efficiency was observed in GR3-A, achieving a grain size of 110 µm with an efficiency of 92 grains/mm<sup>3</sup>/ppm B. Although the microstructures were similar in all castings, the GR3 series showed the best results. When comparing GR3-A to GR3-B, it was found that their grain sizes were very similar, but the inclusions at the grain boundaries were fewer in GR3-A. The superior performance of GR3-A (110 µm at 0.33 kg/t) compared to GR1-B (124 µm at 1.48 kg/t) is likely due to optimized Ti/B ratios, which enhance heterogeneous nucleation efficiency, as supported by findings on Al<sub>3</sub>Ti layer formation [16]. This contrasts with the use of Mg-Ce additives, which achieved 90 µm in Al-7Si but required higher addition rates [22].

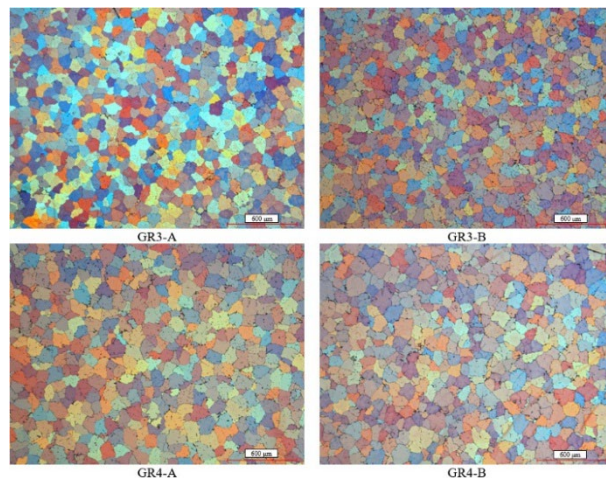


Fig. 8. Microstructure Images of GR3 and GR4 Castings

Grain size measurements were conducted through microscopic analysis of cast samples. For each casting (GR1, GR2, GR3, GR4), images from at least five distinct regions were analyzed using a Nikon Eclipse MA200 microscope. Grain sizes were calculated using the intercept method in accordance with ASTM E112-13 standards [28]. In this method, the number of grain boundary intersections along randomly selected lines was counted, and the average grain size (L) was determined in millimeters. Grain size variance was quantified as the standard deviation (σ) of the measured grain sizes for each casting. The standard deviation was calculated using the following equation:

$$\sigma = \sqrt{\frac{\sum_{i=1}^n (x_i - \bar{x})^2}{n-1}} \quad (3)$$

Where (x<sub>i</sub>) represents individual grain size measurements, ( $\bar{x}$ ) is the mean grain size, and (n) is the number of measurements. For instance, in the GR3-A casting, grain size measurements (approximately 110 µm) from five regions yielded a standard deviation of ±8 µm. Similarly, standard deviations were computed for other castings, and these results were incorporated as error bars in Figure 5.

Figure 5 illustrates the relationship between addition rate and grain size, with error bars representing the grain size variance for each casting. The error bars correspond to ±1 standard deviation, clearly indicating the uncertainty in the measurements. For example, the GR3-A casting, with an addition rate of 0.33 kg/t and a grain size of 110 µm, exhibits an error bar of ±8 µm, corresponding to a range of 102–118 µm. This reflects the repeatability of the measurements and the influence of minor variations in casting conditions.

Grain size measurements adhered to ASTM E112-13, ensuring accurate and reproducible results [28]. This standard provides a robust framework for metallographic grain size determination. As noted in the manuscript, grain sizes measured in furnace samples correlate with those in billets, with billet grain sizes typically being 40–70 µm larger than furnace sample measurements. Standard measurement positions (25–30 mm from the billet surface or at mid-radius) were considered. For the GR3-A casting, a furnace sample grain size of 110 µm corresponds to an estimated billet

grain size of approximately 150–180  $\mu\text{m}$ . These values fall below the 200  $\mu\text{m}$  threshold commonly cited for effective grain refinement, aligning with industrial standards [12, 13].

Grain size deviations may arise from variations in casting conditions, such as cooling rate or alloy composition, as well as slight differences in grain refiner addition rates. For instance, GR1 and GR2 castings, which utilized higher addition rates (around 1.5 kg/t), exhibited larger standard deviations ( $\pm 12 \mu\text{m}$ ), suggesting reduced microstructural homogeneity. In contrast, GR3 and GR4 castings, with lower addition rates (0.33–0.76 kg/t), demonstrated smaller standard deviations ( $\pm 8\text{--}10 \mu\text{m}$ ), indicating a more uniform microstructure.

The analysis of grain size variance confirms that GR3 and GR4 castings achieve high efficiency with lower addition rates. Notably, the GR3-A casting, with a 0.33 kg/t addition rate, produced a grain size of 110  $\mu\text{m}$  with a standard deviation of  $\pm 8 \mu\text{m}$ , highlighting both cost-effectiveness and efficiency. This finding is consistent with the tetrakaidecahedron model, which quantifies grain refiner efficiency based on boride particle nucleation [27]. The model suggests that low boron concentrations (10–20 ppm) can suffice for effective nucleation, as supported by previous findings [18].

The literature widely acknowledges the efficacy of Al-Ti-B master alloys in grain refinement [5, 12, 13]. However, this study's observation that GR3 and GR4 achieve comparable or smaller grain sizes with lower addition rates offers significant implications for industrial cost optimization. Zhang et al. (2025) note that Al-Ti-B promotes heterogeneous nucleation, but excessive addition rates may reduce efficiency, a trend observed in the lower efficiency of GR1 and GR2 castings with high addition rates (1.5 kg/t). This underscores the importance of optimizing addition rates to balance cost and performance.

Grain size deviations are influenced by casting parameters, warranting further investigation into factors such as cooling rate and alloy composition. For example, it has been demonstrated that the Al<sub>3</sub>Ti layer on TiB<sub>2</sub> particles significantly affects nucleation [16]. The lower deviations in GR3 and GR4 castings suggest that their Ti/B ratios may be better optimized, a hypothesis that merits further exploration in future studies to elucidate nucleation mechanisms.

The impact of grain refinement on mechanical properties is also noteworthy. It was reported that a 69% reduction in grain size in AA6082 alloys resulted in a 17% increase in mechanical strength [20]. The 110  $\mu\text{m}$  grain size achieved in GR3-A likely contributes to similar mechanical enhancements, though additional mechanical testing is required to confirm this. Future research should focus on optimizing Ti/B ratios and exploring alternative grain refinement methods to further enhance the mechanical properties and castability of aluminum alloys.

In summary, this study demonstrates that lower addition rates, particularly 0.33 kg/t in GR3-A, yield smaller grain sizes and higher efficiency. The incorporation of grain size variance and error bars, calculated per ASTM E112-13, enhances the reliability of the results. These findings pave the way for more economical and environmentally sustainable grain refinement practices in aluminum billet production.

## 4. Conclusions

This study investigated the effects of different grain refiners and addition rates on the chemical composition, grain size, and efficiency of 6082 aluminum alloy castings. The results from chemical analysis and microstructure examinations revealed significant changes in the alloy's properties due to the addition of grain refiners. The incorporation of grain size variance and error bars, calculated per ASTM E112-13, enhances the reliability of the results and supports the feasibility of low addition rates for industrial applications.

The enhanced efficiency at low addition rates is attributed to optimized nucleation driven by boride particles, enabling fine, homogeneous microstructures with minimal material usage. Detailed chemical analysis revealed that the incorporation of grain refiners resulted in clearly observable shifts in the concentration levels of titanium (Ti) and boron (B) within the material. However, the recovery rates for some additions were lower than expected, particularly in cases with low addition rates (GR3 and GR4), which yielded more efficient results. These results indicate that lower addition rates improve efficiency, while higher rates often yield diminishing returns. Specifically, in the GR3-A casting, a 0.33 kg/t addition rate resulted in a grain size of 110  $\mu\text{m}$ , while a 0.76 kg/t addition rate reduced the grain size to 105  $\mu\text{m}$ . This suggests that excessive addition rates are unnecessary and that a 0.33 kg/t addition is sufficient for achieving the desired grain refinement.

Microstructure analysis confirmed the effectiveness of the grain refiners used in the castings. The grain sizes obtained were inversely proportional to the addition rates. Notably, the GR3 and GR4 castings, which used lower addition rates, achieved grain sizes similar to or even smaller than those obtained with higher addition rates. These findings highlight that lower addition rates can lead to higher efficiency in grain refinement.

In conclusion, the findings of this study emphasize the need for optimization in the use of grain refiners in aluminum alloys. Lower addition rates result in smaller grain sizes and higher efficiency, while excessive additions often fail to provide the desired benefits. This suggests that more efficient and cost-effective methods can be applied in industrial casting processes. Future research should focus on optimizing grain refiner addition rates and exploring alternative refinement methods to significantly enhance the mechanical properties and castability of aluminum alloys.

## Acknowledgment

This research was supported by Sistem Alüminyum San. ve Tic. A.Ş.

## References

- [1] Johnson, W.A. (1990). Molybdenum. In: *Metals Handbook: Vol. 2. Properties and selection: nonferrous alloys and special-purpose materials* (pp. 574). ASM International, Materials Park, OH.
- [2] Totten, G.E., MacKenzie, D.S. (2003). *Handbook of Aluminum: Volume 2: Alloy Production and Materials*

- Manufacturing*. CRC Press, <https://doi.org/10.1201/9780203912607>.
- [3] Kvackaj, T. (2011). *Aluminium Alloys: Theory and Applications*. BoD-Books on Demand. <https://doi.org/10.5772/576>.
- [4] ASM International Handbook Committee. (1991). Heat treating of aluminum alloys. In *ASM Handbook: Heat Treating* (Vol. 4, pp. 841–879). ASM International, Materials Park, OH. <https://doi.org/10.1361/asmhba0001205>.
- [5] Zhang, X., Le, Q., Zhao, D., Jiang, Y., Wang, Y., Wang, T. & Liao, Q. (2025). Research status and prospect of grain refinement in aluminum alloy. *Journal of Materials Research and Technology*. 34, 1880-1893. <https://doi.org/10.1016/j.jmrt.2024.12.205>.
- [6] Tunca, B., Ince, B. & Deniz, D. (2025). Advancements in refining techniques for improving liquid metal quality in aluminum alloys. *Engineering Research: Perspectives on Recent Advances*. 4, 157-176. <https://doi.org/10.9734/bpi/erpra/v4/4481>.
- [7] Tunca, B., Ince, B. & Deniz, D. (2025). Enhancing liquid metal quality in aluminum alloys: A study on refining techniques. *Journal of Engineering Research and Reports*. 27(2), 104-113. <https://doi.org/10.9734/jerr/2025/v27i21398>.
- [8] Liu, X., Wang, B., Li, Q., Wang, J., Xue, C., Yang, X. & Liu, X. (2022). Quantifying the effects of grain refiners (AlTiB and Y) on microstructure and properties in W319 alloys. *Materials Today Communications*. 33, 104671, 1-12. <https://doi.org/10.1016/j.mtcomm.2022.104671>.
- [9] Quedsted, T.E. & Greer, A.L. (2005). Grain refinement of Al alloys: Mechanisms determining as-cast grain size in directional solidification. *Acta Materialia*. 53(17), 4643-4653. <https://doi.org/10.1016/j.actamat.2005.06.018>.
- [10] McCartney, D.G. (1989). Grain refining of aluminium and its alloys using inoculants. *International Materials Reviews*. 34(1), 247-260. <https://doi.org/10.1179/imr.1989.34.1.247>.
- [11] Arnberg, L., Backerud, L. & Klang, H. (1982). Evidence of metastable phase in Al-Ti-(B) system. *Metals Technology*. 9(1), 14-17.
- [12] Schumacher, P., Greer, A.L., Worth, J., Evans, P.V., Kearns, M.A., Fisher, P. & Green, A.H. (1998). New studies of nucleation mechanisms in aluminium alloys: Implications for grain refinement practice. *Materials Science and Technology*. 14(5), 394-404. <https://doi.org/10.1179/mst.1998.14.5.394>.
- [13] Murty, B.S. & Kori, S.A., Chakraborty, M. (2002). Grain refinement of aluminium and its alloys by heterogeneous nucleation and alloying. *International Materials Reviews*. 47(1), 3-29. <https://doi.org/10.1179/095066001225001049>.
- [14] Lee, M.S., Terry, B.S. & Grieveson, P. (1993). Interfacial phenomena in the reactions of Al and Al-Ti melts with KF-AIF<sub>3</sub> and NaF-AIF<sub>3</sub> melts. *Metallurgical Transactions B*. 24, 955-961. <https://doi.org/10.1007/BF02660987>.
- [15] Lee, Y.C., Dahle, A.K., StJohn, D.H. & Hutt, J.E.C. (1999). The effect of grain refinement and silicon content on grain formation in hypoeutectic Al-Si alloys. *Materials Science and Engineering: A*. 259(1), 43-52. [https://doi.org/10.1016/S0921-5093\(98\)00884-3](https://doi.org/10.1016/S0921-5093(98)00884-3).
- [16] Li, J., Hage, F.S., Ramasse, Q.M. & Schumacher, P. (2021) The nucleation sequence of  $\alpha$ -Al on TiB<sub>2</sub> particles in Al-Cu alloys. *Acta Materialia*. 206, 116652, 1-9. <https://doi.org/10.1016/j.actamat.2021.116652>.
- [17] Guan, R.G. & Tie, D. (2017). A review on grain refinement of aluminum alloys: Progresses, challenges and prospects. *Acta Metallurgica Sinica (English Letters)*. 30(5), 409-432. <https://doi.org/10.1007/s40195-017-0565-8>.
- [18] Sigworth, G.K. & Kuhn, T.A. (2007). Grain refinement of aluminum casting alloys. *International Journal of Metalcasting*. 1(1), 31-40. <https://doi.org/10.1007/BF03355416>.
- [19] Jones, G.P. & Pearson, J. (1976). Factors affecting the grain-refinement of aluminum using titanium and boron additives. *Metallurgical Transactions B*. 7(2), 223-234. <https://doi.org/10.1007/BF02654921>.
- [20] Izcankurtaran, D., Tunca, B. & Karatay, G. (2021). Investigation of the effect of grain refinement on the mechanical properties of 6082 aluminium alloy. *Open Journal of Applied Sciences*. 11(6), 699-706. <https://doi.org/10.4236/ojapps.2021.116051>.
- [21] Easton, M.A., Qian, M., Prasad, A. & StJohn, D.H. (2016). Recent advances in grain refinement of light metals and alloys. *Current Opinion in Solid State and Materials Science*. 20(1), 13-24. <https://doi.org/10.1016/j.cossms.2015.10.001>.
- [22] Zhao, J., Shi, M., Wang, Z. & Xu, L. (2019). Effect of a new grain refiner (Al-Ti-Mg-Ce) on hardness, tensile, and impact properties of Al-7Si alloy. *Metals*. 9(2), 228, 1-17. <https://doi.org/10.3390/met9020228>.
- [23] Li, D., Zhao, K., Liu, G., Han, M., Liu, S. & Liu, X. (2023). Revealing the correlation of microstructure configuration and mechanical properties of Al-Si-Mg alloy reinforced by C-doped TiB<sub>2</sub> and SiC. *Materials & Design*. 226, 111694, 1-16. <https://doi.org/10.1016/j.matdes.2023.111694>.
- [24] Prema, S., Chandrashekharaiah, T.M. & Begum P.F. (2019). Effect of grain refiners and/or modifiers on the microstructure and mechanical properties of Al-Si alloy (LM6). *Materials Science Forum*. 969, 794-799. <https://doi.org/10.4028/www.scientific.net/MSF.969.794>.
- [25] Zhang, Y., Ji, S. & Fan, Z. (2017). Improvement of mechanical properties of Al-Si alloy with effective grain refinement by in-situ integrated Al<sub>2</sub>TiB-Mg refiner. *Journal of Alloys and Compounds*. 710, 166-171. <https://doi.org/10.1016/j.jallcom.2017.03.244>.
- [26] Hatić, V., Mavrič, B. & Šarler, B. (2020). Simulation of macrosegregation in direct-chill casting- A model based on meshless diffuse approximate method. *Engineering Analysis with Boundary Elements*. 113, 191-203. <https://doi.org/10.1016/j.enganbound.2019.12.006>.
- [27] Greer, A.I., Bunn, A.M., Tronche, A., Evans, P.V. & Bristow, D.J. (2020). Modelling of inoculation of metallic melts: Application to grain refinement of aluminium by Al-Ti-B. *Acta Materialia*. 48(11), 2823-2835. [https://doi.org/10.1016/S1359-6454\(00\)00094-X](https://doi.org/10.1016/S1359-6454(00)00094-X).
- [28] ASTM E112-13, Standard Test Methods for Determining Average Grain Size, ASTM International, West Conshohocken, PA, 2013.